Comparison of Methods for Determining the Mechanical Properties of Semiconducting Polymer Films for Stretchable Electronics

Daniel Rodriquez,[†,∥] Jae-Han Kim,[‡,∥] Samuel E. Root,[†] Zhuping Fei,[§] Pierre Boufflet,[§] Martin Heeney,[§] Taek-Soo Kim,[*,‡] and Darren J. Lipomi[*,†]

[†]Department of NanoEngineering, University of California, San Diego 9500 Gilman Drive, Mail Code 0448, La Jolla, California 92093-0448, United States

[‡]Department of Mechanical Engineering, Korea Advanced Institute of Science and Technology (KAIST), Yuseong-gu, Daejeon 34141, Korea

[§]Department of Chemistry and Centre for Plastic Electronics, Imperial College London, Exhibition Rd, London, SW7 2AZ, United Kingdom

Ⓢ *Supporting Information*
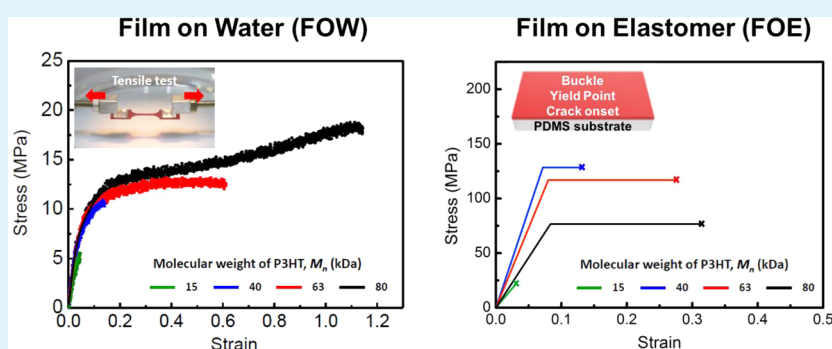
ABSTRACT: This paper describes a comparison of two characterization techniques for determining the mechanical properties of thin-film organic semiconductors for applications in soft electronics. In the first method, the film is supported by water (film-on-water, FOW), and a stress–strain curve is obtained using a direct tensile test. In the second method, the film is supported by an elastomer (film-on-elastomer, FOE), and is subjected to three tests to reconstruct the key features of the stress–strain curve: the buckling test (tensile modulus), the onset of buckling (yield point), and the crack-onset strain (strain at fracture). The specimens used for the comparison are four poly(3-hexylthiophene) (P3HT) samples of increasing molecular weight (M_n = 15, 40, 63, and 80 kDa). The methods produced qualitatively similar results for mechanical properties including the tensile modulus, the yield point, and the strain at fracture. The agreement was not quantitative because of differences in mode of loading (tension vs compression), strain rate, and processing between the two methods. Experimental results are corroborated by coarse-grained molecular dynamics simulations, which lead to the conclusion that in low molecular weight samples (M_n = 15 kDa), fracture occurs by chain pullout. Conversely, in high molecular weight samples (M_n > 25 kDa), entanglements concentrate the stress to few chains; this concentration is consistent with chain scission as the dominant mode of fracture. Our results provide a basis for comparing mechanical properties that have been measured by these two techniques, and provide mechanistic insight into fracture modes in this class of materials.

KEYWORDS: mechanical properties, organic semiconductors, stretchable electronics, P3HT, buckling-based metrology, film on water, film on elastomer, thin films

INTRODUCTION

The mechanical properties of thin-film organic semiconductors play an important role in the durability of organic electronic devices such as organic solar cells, thin-film transistors, light-emitting devices, and biosensors.[1−4] For example, low tensile moduli reduce interfacial stresses and are necessary to achieve "mechanical invisibility" in wearable patch-like devices.[5] High ductility and toughness, however, will increase the lifetimes of devices against fracture and enable stretching and bonding of devices to curve surfaces of buildings, vehicles, and body parts.[6]

Recently, stretchability in organic semiconductors has been achieved by modification of the molecular structure to include chemical cross-linking groups or by surface embedding in an elastomer.[7,8] Since organic semiconductors are usually cast into films as thin as a few tens of nanometers thick, it is challenging to obtain mechanical information using conventional methods,

such as pull testing of freestanding samples.[9] Moreover, the mechanical properties of thin films are not necessarily the same as those of bulk samples.[10] This challenge has led to the development of methods for determining the mechanical properties of thin films of semiconducting polymers that do not require preparation of bulk samples (laboratory-scale syntheses of new materials usually do not produce a large enough yield).[11−13]

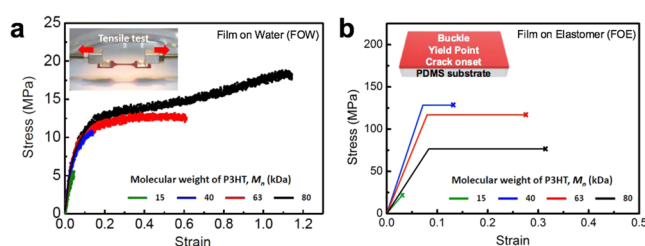The purpose of this work is to compare two of these experimental methods (Figure 1), and to compare the results

Figure 1. Comparison of stress−strain behavior measured for film-on-water and film-on-elastomer methods. (a) Engineering stress−strain curves of P3HT thin films with increasing molecular weight (15, 41, 64, and 80 kDa) determined by FOW methods. (b) Approximated stress−strain curves for the same P3HT thin films determined by FOE methods.

with a simulated stress−strain curve produced by a coarse-grained molecular dynamics simulation.[14] The first method, which we refer to as "film-on-water" (FOW), is similar to a conventional pull test, except that the thin-film sample is suspended on water.[1,12] This method produces a stress−strain curve like that of a conventional pull test. The second method, which we refer to as "film-on-elastomer" (FOE), combines three measurements that together can be used to approximate the stress−strain curve.[15] The three measurements used in the FOE method are (1) the buckling method to obtain the tensile modulus, (2) the onset of surface wrinkles to approximate the yield point, and (3) the crack-onset strain to approximate the strain at fracture.[15−17] We chose the widely studied regioregular poly(3-hexylthiophene) (P3HT) of four different molecular weights to serve as the subject of our comparison of the two methods. While we found good qualitative agreement between the two methods in showing increasing resistance to fracture with increasing molecular weight, the agreement in tensile modulus was poor. Differences in the values of mechanical properties produced by these methods are attributed to the ways in which the films are deformed and the extent to which defects and heterogeneity in the films influence the force required to deform them. The results we report may interest researchers concerned with metrology of thin-film polymers and increasing the lifetimes of devices for stretchable, ultraflexible, and mechanically robust applications.

EXPERIMENTAL SECTION

Molecular Weight of Poly(3-hexylthiophene) (P3HT). We selected P3HT for this study because of its well-known microstructure, thermal transitions, and optoelectronic properties in thin-film transistors, solar cells, and biosensors.[18] Of particular importance for this study is its quasi-living synthetic mechanism using the Grignard metathesis polymerization, which affords excellent control over molecular weight and dispersity.[19] The molecular weight, in turn, has a profound effect on microstructure and optoelectronic properties. For example, an early study by Kline et al. showed an increase in field-

effect mobility with molecular weight from a value of 1.7×10^{-6} cm^2 V^{-1} s^{-1} at 3.2 kDa to 9.4×10^{-6} cm^2 V^{-1} s^{-1} at 36.5 kDa.[20] This change in mobility was correlated to significant changes in the morphology of the system, from rod-like structures in the 3.2 kDa sample to isotropic nodule structures in the 36.5 kDa film, as seen in AFM images.[20] X-ray diffraction measurements revealed that the 3.2 kDa sample had a greater signal intensity for the ⟨100⟩ peak than the 36.5 kDa sample, which indicated a higher degree of crystallinity, albeit lower mobility.[20] However, the mobility of the low molecular weight sample could be increased by manipulating the morphology through annealing or using a solvent with a high boiling point.[21] Recent studies have shown that the mobility of P3HT continues to increase with molecular weight until it saturates at a critical value.[22] This critical point occurs once the molecular weight is high enough such that the lattice disorder becomes independent of polymer chain length.[22] We note that values of molecular weight obtained from gel-permeation chromatography (GPC) using polystyrene standards overestimate the weight obtained by MALDI-TOF-MS or NMR by a value of approximately 1.67.[23]

Effect of Molecular Weight on the Mechanical Properties of P3HT. While the mechanical properties of P3HT as a function of molecular weight have been measured before, the results were obtained using bulk samples,[9] or nanodynamic mechanical analysis,[24] as opposed to measurement on thin films. In general, increasing the molecular weight of P3HT increases the ductility (strain at fracture) and toughness (total energy density absorbed by the material at the point of fracture).[9] The most important microstructural characteristic that influences the mechanical properties of polymers with increasing molecular weight is the density of entanglements.[25] An entanglement is a physical linking of polymer chains, and a consequence of the fact that two chains can slide past but not cross one another.[25] Another effect is that at higher molecular weights, stiff crystallites are connected by tie molecules.[22] Using traditional pull testing, Koch et al. measured the mechanical properties of bulk samples of P3HT tapes prepared by melt casting in a uniaxial tensile test. The authors reported that the stress at failure increased from 8 to 24 MPa and the elongation improved from ~10% to ~300% in the 20 and 110 kDa samples, respectively.[9] The role of entanglements was established by measuring the specific viscosity of each solution. The authors determined the critical molecular weight at which the chains become entangled to be ~35 kDa, as indicated by a sharp increase in viscosity.[9] Moreover, the melting temperature and enthalpy of fusion saturated after ~30 kDa, which further provides evidence for the onset of chain entanglement at this molecular weight.[9] The resistance to fracture of thin films of high molecular weight P3HT has also been measured using a four-point bend test. For example, Bruner et al. showed that as the molecular weight of P3HT increased, the cohesive energy of composites of P3HT with the fullerene derivative phenyl-C$_{61}$-butyric acid methyl ester ([60]PCBM) exhibited an increase from ~1−2 J m^{-2} at 28 kDa to nearly ~17 J m^{-2} at 100 kDa.[26]

Film-On-Water (FOW) Measurements. The FOW technique is a pseudo free-standing tensile test that exploits the high surface tension of water, 73 mN m^{-1}, to suspend thin films on the water surface.[12] The low viscosity of water allows for unimpeded sliding of the films on the water surface; this scenario is ideal for replicating a free-standing tensile test.[12] Once the film is floated on the water surface, it is attached to the load grips using small PDMS slabs that make van der Waals adhesion with the load cell and the thin film. The film is then strained at a strain rate of $\sim 0.3 \times 10^{-3}$ s^{-1} until failure of the film to produce a stress−strain curve. This method combines the advantages of free-standing tensile tests with those of substrate-supported tests. That is, it provides a direct measurement of the mechanical properties while providing a means of manipulating ultrathin films which would otherwise collapse upon themselves in air.

Film-On-Elastomer (FOE) Measurements. FOE methods comprise three separate measurements that collectively approximate a stress−strain curve of a thin film and allow the rough estimation of the energies of deformation, i.e., resilience and toughness. The three tests are mechanical buckling to measure the tensile modulus, onset of buckling to measure the yield point, and stretching until failure to
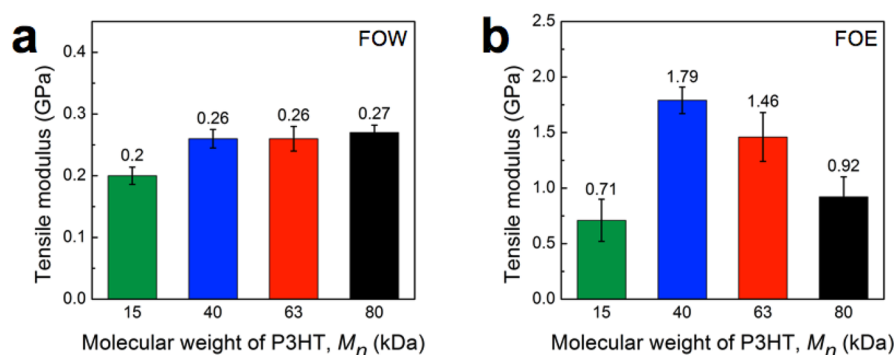
Figure 2. Tensile moduli of P3HT thin films with a range of molecular weight. (a) As measured by FOW methods. (b) As measured by FOE methods.

determine the crack-onset strain.[15−17] Mechanical buckling, also known as surface wrinkling, is a well-documented method of measuring the tensile modulus of otherwise difficult-to-measure thin film systems such as organic semiconductors, polymer brushes, and nanostructured materials supported by an elastomeric substrate.[10] This technique is useful over a wide range of film thicknesses (20 to 500 nm) and tensile moduli and is sufficiently sensitive to detect modulus anisotropy in polymer thin films.[27−30] The tensile moduli of materials obtained from this method agree well with those reported from traditional methods and dynamic mechanical analysis.[31−33] Onset of buckling is an FOE method that detects the formation of surface wrinkles to determine the yield point of the film. The method is performed by cyclically, and incrementally, straining and relaxing a thin film on an elastomeric substrate (i.e., 0% → 1% → 0% → 2% → 0% → 3% → 0%, etc.). Once the yield point is reached, the film is plastically deformed and upon relaxation the film is compressed and buckles form on the surface. The onset of buckles in the film manifests as a diffraction pattern obtained using a laser, or can be visibly seen in a microscope under favorable conditions.[34] Crack-onset strain measurements in the FOE method are used to determine the strain at which the material begins to fail. Briefly, a thin-film material is transferred to an elastomeric substrate and is incrementally strained until the formation of pinholes or cracks appear in the film. While the FOE methods were introduced as an alternative to nanoindentation and tensile tests of free-standing samples, the FOE methods are time-consuming and use significantly more material than FOW methods.

Molecular Dynamics (MD). MD simulations can be used to predict the nanoscale structural and mechanical properties of polymeric materials.[35] They probe mechanical phenomena on a level of detail that is impossible to characterize experimentally. Although high molecular weight polymers are exceedingly time-consuming to simulate using atomistic models, detailed coarse-grained models can be used to simulate highly entangled polymeric systems.[36−38] To complement our experimental study, we employed a three-site model for P3HT developed by Huang and co-workers to simulate the effect of molecular weight on structure, entanglement and response to uniaxial tensile loading. We have previously demonstrated that this model predicts the mechanical properties of P3HT accurately.[38]

■ RESULTS AND DISCUSSION

Tensile Modulus. We measured the tensile modulus of each film using two different methods, FOW and FOE, and compared the results (Figure 2a,b). We can see that the FOE method produced values for tensile moduli that were 3−7 times higher than those produced by FOW. However, both sets of values were in the range of values reported in literature, 0.22 to 1.33 GPa.[16,39−43] In the FOW tests, the modulus was constant for samples ≥40 kDa. Similar tendencies for the modulus of P3HT to saturate with increasing molecular weight have been reported using a molecular dynamics simulation.[35] Tummala et al. showed that the modulus does not change significantly

above the entanglement chain length since the modulus is the stress response in the initially elastic regime.[35] In the FOE method, the moduli increased as the molecular weight increased from 15 kDa to 40 kDa, and decreased for samples >40 kDa. We hypothesize that the polymer chains are well packed and confined up to 40 kDa (just above the entanglement chain length). However, above the entanglement length, polymer chains exhibit slower reptation dynamics and cannot pack as efficiently. This phenomenon results in increased free volume of the amorphous domains and softer behavior in compression tests. For both the FOW and FOE method, the 15 kDa sample exhibited the lowest modulus and greatest brittleness. The brittleness observed for 15 kDa is consistent with the fact that the molecular weight is smaller than the previously determined entanglement molecular weight for P3HT of 25 kDa, as determined by GPC.[9]

We attribute the difference in values for tensile modulus obtained using the FOW and FOE methods to three factors: (1) voids in the film which create a different stress response under tension vs compression, (2) inhomogeneities in thickness (surface roughness), and (3) strain rate. It is often found that materials measured in compression exhibit higher moduli than those measured in tension.[44] For example, a study by Johnston et al. reported the tensile modulus of PDMS cured at room temperature to be 1.32 ± 0.07 MPa, the same sample exhibited a compressive modulus of 186.9 ± 5.39 MPa.[45] Similar results have been reported for polyethylene and epoxy resins.[46,47] In the FOW method, the films experience tensile stress, whereas the buckling technique used in the FOE method produces compressive stress. Variation in the stress response of the materials under these two modes of deformation can occur for two reasons. The first is the presence of imperfections, voids, and pinholes arising from free volume in the polymer network or processing of the films. Under tension, these imperfections will grow or elongate and can manifest as a reduction in the modulus, whereas in compression voids and pinholes will be closed; closing of the pinholes minimizes their effects and leads to a higher modulus (Figure 3).[44]

The second factor that may contribute to lower values for modulus in the FOW method is surface roughness and imperfections. That is, in a thin film, the roughness may be a significant fraction of the total thickness of the film. We used atomic force microscopy (AFM) to quantify the degree of surface roughness (Figure 4). Overall, it shows similar surface morphology in all the samples. The peak-to-valley roughness, R_{pv}, was around 25−34 nm, which is 13−17% of total films thickness (~200 nm). The inhohogeneities of film thickness
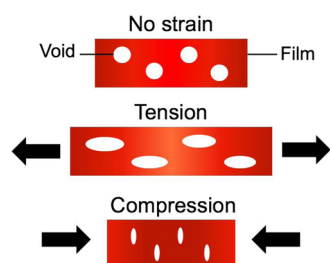
Figure 3. Illustration depicting the effect of tensile and compressive stresses on voids, pinholes, and imperfections in a thin film. Under tension defects will grow and become larger, in compression this effect is reversed and the defects shrink.

Figure 5. Stress−strain curves of 63 kDa P3HT tested using two different strain rates. The FOW pull test conducted using the faster strain rate produced a 2× larger apparent tensile modulus.

from the high peak-to-valley distances can cause the stress concentration in the thinnest regions of the film under tension, and the concentration of the stress would thus produce lower values for modulus and premature failure. In compression this effect is mitigated because the valleys at the film surface will be closed.

In any stress−strain measurement, the strain rate effects the apparent modulus. Generally, higher strain rates lead to higher moduli.[44] To illustrate this effect, we tested a 63 kDa P3HT sample at a fast and slow strain rate in the FOW setup (Figure 5). The FOW tensile test conducted at a relatively slow strain rate of 0.3×10^{-3} s^{-1} produced a modulus value of 0.261 GPa. The fast FOW test had a strain rate of 3.0×10^{-3} s^{-1} and the modulus obtained was 0.438 GPa, which is almost 2× larger than the value obtained using the slow test. A similar experiment was performed using the FOE method where a sample was compressed at a relatively slow rate of 0.3×10^{-1} s^{-1} on a linear actuator and a fast rate by releasing the strain instantaneously, but there was no significant change in the buckling wavelength with varying strain rate. We hypothesize the strain rate effects in tensile loading are largely responsible for the differences in the moduli reported by the two methods, FOW and FOE. In the FOW test the strain rate was slow at 0.3×10^{-3} s^{-1} however, a faster strain rate would have produced a larger tensile modulus. Collectively the effects from varying strain rate, inhomogenieties in film thickness, and void space in the films behaving differently in tension versus compression lead to a larger tensile modulus being reported in compressive FOE buckling measurements than those reported in free-standing FOW tensile tests.

Ductility. Both methods show good qualitative agreement in the increase of ductility of the films with increasing molecular weight (Table 1). The differences in the absolute values of the strain at failure arise from the labeling of the failure point in FOE methods. In the FOW method, the strain at failure is the point at which the film is completely ruptured; in the FOE
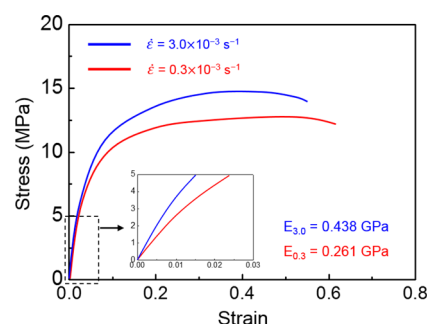
method, the strain at failure is labeled as the onset of cracks or pinholes in the film. The strain at which the film completely ruptures (bifurcates) in the FOE method would be much higher than in the FOW method. The great extent to which a film on an elastomeric substrate can be stretched is not a true represenation of the strain at which a freestanding film would fail. This difference is due to the film being supported by an elastomeric substrate which redistributes stress to the film (as opposed to in the FOW method, where stress is concentrated to the defects and thin areas). The mechanical behavior of the elastomeric substrate also plays an important role in the crack behavior observed in the thin films. A stiff substrate with an elastic modulus closer to that of the P3HT thin film lead to the onset of cracks at a higher strain, compared to a softer elastomer which cracked at relatively lower strains due to the greater mismatch in the elastic modulus. (Figure S1 of the Supporting Information). To mitigate this effect, it is best to select a substrate that is close to the modulus of the thin film to help reduce interfacial stresses while maintaining sufficient adhesion for the transfer of the film to the substrate. It was expected that the ductility of the films would increase with molecular weight for two reasons: (1) at higher molecular weight there is an increase in the degree of interchain π-stacking in the crystalline regions of the film which increases the number of van-der-Waals bonds needed to be broken for chain pullout to occur and (2) in the amorphous regime there is an increase in the number of intrachain folds and physical linking of the polymer chains which makes disentanglement of chains increasingly difficult.[26] We hypothesize that at low molecular weight the polymer film has a low density of entanglements and cracking occurs by chain pullout. At high molecular weight there is a high density of entanglements and cracking occurs by chain scission.

Aggregation Behavior. Ultraviolet/visible (UV/vis) spectroscopy measurements were used to measure how the
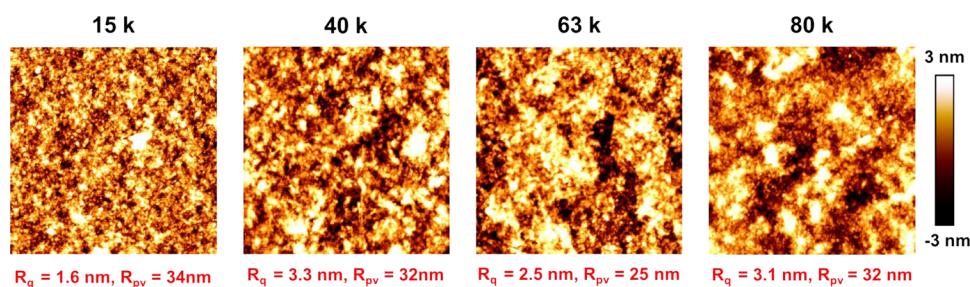

R_q = 1.6 nm, R_{pv} = 34nm R_q = 3.3 nm, R_{pv} = 32nm R_q = 2.5 nm, R_{pv} = 25 nm R_q = 3.1 nm, R_{pv} = 32 nm

Figure 4. AFM images showing the surface morphology of P3HT with increasing molecular weight. Scan area was $5 \times 5 \ \mu m^2$.

Table 1. Tabulated Values of the Mechanical Properties of P3HT Films as a Function of Molecular Weight

| FOW methods				
M_n (kDa)	tensile modulus (GPa)	strain at fracture (%)	toughness (kJ/m^3)	tensile strength (MPa)
15	0.203 ± 0.014	4.5 ± 0.3	0.14 ± 0.01	4.5 ± 0.3
40	0.263 ± 0.015	13.0 ± 1.2	0.99 ± 0.08	10.5 ± 0.5
63	0.261 ± 0.020	58.7 ± 6.5	6.80 ± 0.78	12.6 ± 0.2
80	0.270 ± 0.012	95.6 ± 7.7	13.17 ± 0.97	17.1 ± 0.6
FOE methods				
M_n (kDa)	tensile modulus (GPa)	crack onset strain (%)	estimated toughness (kJ/m^3)	tensile strength (MPa)
15	0.71 ± 0.19	2.83 ± 0.41	0.85 ± 0.21	
40	1.79 ± 0.12	12.83 ± 1.72	11.87 ± 3.77	
63	1.46 ± 0.22	27.33 ± 4.37	27.25 ± 7.62	
80	0.92 ± 0.18	31.17 ± 11.67	20.69 ± 9.89	
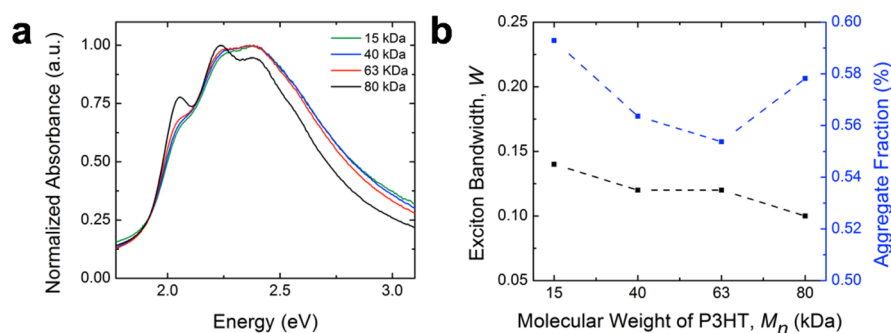
Figure 6. (a) UV/vis spectra showing the normalized absorbance of P3HT thin films with increasing M_n. (b) Exciton bandwidth, W, of the P3HT thin films as determined by the weakly interacting H-aggregate model. W is inversely correlated with conjugation length.

optoelectronic properties changed with molecular weight (Figure 6a). In particular we sought to analyze the degree of aggregation present in the semicrystalline P3HT thin films. The absorption of weakly interacting H-aggregates is determined by coupled electronic-vibrational (vibronic) energy transitions. Two effects were observed: (1) there was a small red shift with increasing molecular weight and (2) the peaks associated with the vibronic progression are the most pronounced for the 80 kDa sample. Similar results have been reported previously by Kline and Zen et al.[21,48] Analysis using the weakly interacting H-aggregate model revealed an increase in the conjugation length of P3HT with increasing molecular weight, as manifested in a decrease in the exciton bandwidth extracted using the weakly interacting H-aggregate model of Spano and co-workers (Figure 6b).[49−52] These results correlate well with the observed feature changes in the UV/vis spectra, that is, longer conjugation length leads to absorption at lower energy.[53] We hypothesize that increased conjugation in a P3HT thin film leads to more resistance to deformation and therefore a higher tensile modulus as observed in Figure 2a. H-aggregate analysis also showed that the 15 kDa sample had the highest fraction of aggregates which is due to the ability of low molecular weight P3HT to form chain extended crystals and distinct lamellae.[9] As the polymer chains become longer the lamellar structures become intermixed in an amorphous network of polymer which decreases the overall fraction of aggregates. However, once the polymer chains become sufficiently long the degree of self-folding grows which is manifested as an increase in the fraction of aggregates as seen in Figure 6b (data points indicated in blue).

Molecular Dynamics Simulations. Coarse-grained molecular dynamics simulations were used to demonstrate the microscopic effects of entanglements on the tensile response. A description of the models and simulation protocols used can be found in our previous publication.[38] We prepared two systems: one with chain lengths equal to the entanglement length, $N_e \approx$ 50 repeat units, and one with high molecular weight chains of 300 repeat units ($\sim 6N_e$). The morphology was prepared to represent a polymer film that was spin coated from a good solvent such as chloroform; it was homogeneous and did not contain voids. To quantify entanglements, a primitive path analysis was performed using the Z1 algorithm of Kröger and co-workers.[54−57] As expected, we found that the low molecular weight system was barely entangled with ~2 interior kinks per chain while the high molecular weight system was highly entangled with ~8 interior kinks per chain. The low molecular weight system (50-mers) was observed to fracture via chain pullout (Figure 7). The high molecular weight system (300-mers) did not crack in the simulations, instead, we observed that the stress was concentrated to relatively few entangled chains (Figure 7). Although the model employed in these simulations did not include the potential for bonds to break, this observation provided evidence that fracture in entangled samples is in fact due to chain scission. The order of magnitude obtained for the tensile modulus (~1 GPa) was in closer agreement with the FOE method than with the FOW method. We attribute this finding to the fast strain rate employed in the simulations, as well as the absence of macroscopic heterogeneities, voids, and thin-film confinement effects.

■ CONCLUSIONS

We compared the results from two different methods (FOW and FOE) of determining the mechanical properties of P3HT thin films as a function of molecular weight. The FOE method produced higher values of the tensile modulus than the FOW method. These results can be attributed to various differences
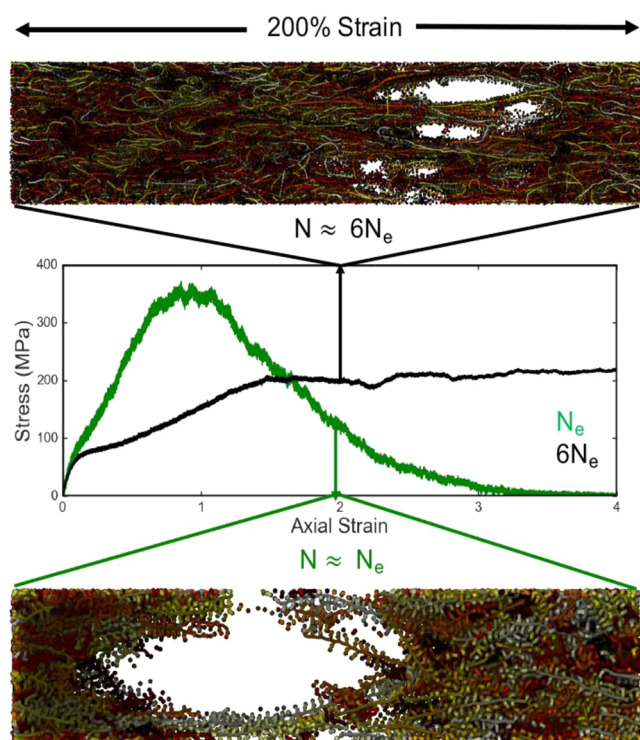
Figure 7. Comparison of uniaxial tensile response between disentangled ($N \approx N_e$) and highly entangled ($N \approx 6N_e$) systems, as computed by coarse-grained MD. Snapshots illustrate a 5 nm slice of the simulation trajectory at 200% strain. Polymers are colored by chain number to make them distinguishable.

between the two metrological techniques including mode of loading (tension vs compression), strain rate, and substrate effects. Complementary coarse-grained MD simulations demonstrate that fracture occurs via chain-pullout in the low molecular weight samples, and provides evidence to support the hypothesis that entangled systems exhibit chain scission as the dominant fracture mechanism. All three methods produced good qualitative agreement in finding the strain at which the films failed and showed an increase in ductility with increasing molecular weight of P3HT. This work revealed that mechanical analysis of thin films is not independent of the method used to study them and offers a point of reference for comparing the mechanical properties of materials measured using a pull test and those using methods involving thin films bonded to elastomers. Furthermore, the results presented here make a strong case for employing pull tests, such as FOW, over FOE based experiments to save time, preserve material, and to obtain the most facile, reliable, and precise measurements of mechanical properties.

ASSOCIATED CONTENT

S Supporting Information

The Supporting Information is available free of charge on the ACS Publications website at DOI: 10.1021/acsami.6b16115.

Figure S1, the experimental details of the synthesis of P3HT; the preparation of substrates and films, FOE and FOW methods; and computational methods (PDF)

AUTHOR INFORMATION

Corresponding Authors
*E-mail: tskim1@kaist.ac.kr (T.-S.K.).

*E-mail: dlipomi@eng.ucsd.edu (D.J.L.).
ORCID
Martin Heeney: 0000-0001-6879-5020
Taek-Soo Kim: 0000-0002-2825-7778
Darren J. Lipomi: 0000-0002-5808-7765
Author Contributions
‖These authors contributed equally.
Notes
The authors declare no competing financial interest.

ACKNOWLEDGMENTS

REFERENCES

(1) Kim, T.; Kim, J.-H.; Kang, T. E.; Lee, C.; Kang, H.; Shin, M.; Wang, C.; Ma, B.; Jeong, U.; Kim, T.-S.; Kim, B. J. Flexible, Highly Efficient All-Polymer Solar Cells. *Nat. Commun.* **2015**, 6 (May), 8547.

(2) Fukuda, K.; Takeda, Y.; Mizukami, M.; Kumaki, D.; Tokito, S. Fully Solution-Processed Flexible Organic Thin Film Transistor Arrays with High Mobility and Exceptional Uniformity. *Sci. Rep.* **2014**, 4, 3947.

(3) Oh, J. Y.; Kim, S.; Baik, H. K.; Jeong, U. Deformable Electronics: Conducting Polymer Dough for Deformable Electronics (Adv. Mater. 22/2016). *Adv. Mater.* **2016**, 28 (22), 4564.

(4) Khan, H. U.; Roberts, M. E.; Johnson, O.; Knoll, W.; Bao, Z. The Effect of pH and DNA Concentration on Organic Thin-Film Transistor Biosensors. *Org. Electron.* **2012**, 13 (3), 519−524.

(5) Kaltenbrunner, M.; Sekitani, T.; Reeder, J.; Yokota, T.; Kuribara, K.; Tokuhara, T.; Drack, M.; Schwödiauer, R.; Graz, I.; Bauer-Gogonea, S.; Bauer, S.; Someya, T. An Ultra-Lightweight Design for Imperceptible Plastic Electronics. *Nature* **2013**, 499 (7459), 458−463.

(6) O'Connor, T. F.; Zaretski, A. V.; Shiravi, B. A.; Savagatrup, S.; Printz, A. D.; Diaz, M. I.; Lipomi, D. J. Stretching and Conformal Bonding of Organic Solar Cells to Hemispherical Surfaces. *Energy Environ. Sci.* **2014**, 7 (1), 370−378.

(7) Wang, G. J. N.; Shaw, L.; Xu, J.; Kurosawa, T.; Schroeder, B. C.; Oh, J. Y.; Benight, S. J.; Bao, Z. Inducing Elasticity through Oligo-Siloxane Crosslinks for Intrinsically Stretchable Semiconducting Polymers. *Adv. Funct. Mater.* **2016**, 26 (40), 7254−7262.

(8) Shin, M.; Oh, J. Y.; Byun, K. E.; Lee, Y. J.; Kim, B.; Baik, H. K.; Park, J. J.; Jeong, U. Polythiophene Nanofibril Bundles Surface-Embedded in Elastomer: A Route to a Highly Stretchable Active Channel Layer. *Adv. Mater.* **2015**, 27 (7), 1255−1261.

(9) Koch, F. P. V.; Rivnay, J.; Foster, S.; Müller, C.; Downing, J. M.; Buchaca-Domingo, E.; Westacott, P.; Yu, L.; Yuan, M.; Baklar, M.; Fei, Z.; Luscombe, C.; McLachlan, M. A.; Heeney, M.; Rumbles, G.; Silva, C.; Salleo, A.; Nelson, J.; Smith, P.; Stingelin, N. The Impact of Molecular Weight on Microstructure and Charge Transport in Semicrystalline Polymer Semiconductors-poly(3-Hexylthiophene), a Model Study. *Prog. Polym. Sci.* **2013**, 38 (12), 1978−1989.

(10) Chung, J. Y.; Nolte, A. J.; Stafford, C. M. Surface Wrinkling: A Versatile Platform for Measuring Thin-Film Properties. *Adv. Mater.* **2011**, 23 (3), 349−368.

(11) Dupont, S. R.; Oliver, M.; Krebs, F. C.; Dauskardt, R. H. Interlayer Adhesion in Roll-to-Roll Processed Flexible Inverted Polymer Solar Cells. *Sol. Energy Mater. Sol. Cells* **2012**, *97*, 171−175.

(12) Kim, J.-H.; Nizami, A.; Hwangbo, Y.; Jang, B.; Lee, H.-J.; Woo, C.-S.; Hyun, S.; Kim, T.-S. Tensile Testing of Ultra-Thin Films on Water Surface. *Nat. Commun.* **2013**, *4*, 2520.

(13) Savagatrup, S.; Printz, A. D.; Rodriquez, D.; Lipomi, D. J. Best of Both Worlds: Conjugated Polymers Exhibiting Good Photovoltaic Behavior and High Tensile Elasticity. *Macromolecules* **2014**, *47* (6), 1981−1992.

(14) Root, S.; Arya, G.; Lipomi, D. J. *Mechanical Properties of Organic Electronic Materials: A Coarse-Grained Molecular Dynamics Study P3HT Amorphous Generation Effect of Alkyl Side-Chain Length Coarse-Grained Models Uniaxial Tensile Deformation Uniaxial Tensile Deformation Support*. **2015**, *117*, 4663.

(15) Printz, A. D.; Zaretski, A. V.; Savagatrup, S.; Chiang, A. S.-C.; Lipomi, D. J. Yield Point of Semiconducting Polymer Films on Stretchable Substrates Determined by Onset of Buckling. *ACS Appl. Mater. Interfaces* **2015**, *7*, 23257−23264.

(16) Savagatrup, S.; Makaram, A. S.; Burke, D. J.; Lipomi, D. J. Mechanical Properties of Conjugated Polymers and Polymer-Fullerene Composites as a Function of Molecular Structure. *Adv. Funct. Mater.* **2014**, *24* (8), 1169−1181.

(17) Rodriquez, D.; Savagatrup, S.; Valle, E.; Proctor, C. M.; McDowell, C.; Bazan, G. C.; Nguyen, T.-Q.; Lipomi, D. J. Mechanical Properties of Solution-Processed Small-Molecule Semiconductor Films. *ACS Appl. Mater. Interfaces* **2016**, *8*, 11649−11657.

(18) Brinkmann, M. Structure and Morphology Control in Thin Films of Regioregular poly(3-Hexylthiophene). *J. Polym. Sci., Part B: Polym. Phys.* **2011**, *49* (17), 1218−1233.

(19) McCullough, R. D. The Chemistry of Conducting Polythiophenes. *Adv. Mater.* **1998**, *10* (2), 93−116.

(20) Kline, R. J.; McGehee, M. D.; Kadnikova, E. N.; Liu, J.; Frechet, J. M. J. Controlling the Field-Effect Mobility of Regioregular Polythiophene by Changing the Molecular Weight. *Adv. Mater.* **2003**, *15* (18), 1519−1522.

(21) Kline, R. J.; Mcgehee, M. D.; Kadnikova, E. N.; Liu, J.; Frechet, J. M. J.; Toney, M. F. The Dependence of Regioregular Poly (3-Hexylthiophene) Film Morphology and Field-Effect Mobility on Molecular Weight. *Macromolecules* **2005**, *38* (8), 3312−3319.

(22) Noriega, R.; Rivnay, J.; Vandewal, K.; Koch, F. P. V; Stingelin, N.; Smith, P.; Toney, M. F.; Salleo, A. A General Relationship between Disorder, Aggregation and Charge Transport in Conjugated Polymers. *Nat. Mater.* **2013**, *12* (11), 1038−1044.

(23) Koch, F. P. V; Smith, P.; Heeney, M. Fibonacci'S Route" To Regioregular Oligo(3-Hexylthiophene)S. *J. Am. Chem. Soc.* **2013**, *135* (37), 13695−13698.

(24) Bruner, C.; Miller, N. C.; McGehee, M. D.; Dauskardt, R. H. Molecular Intercalation and Cohesion of Organic Bulk Heterojunction Photovoltaic Devices. *Adv. Funct. Mater.* **2013**, *23*, 2863−2871.

(25) Likhtman, A. E.; Ponmurugan, M. Microscopic Definition of Polymer Entanglements. *Macromolecules* **2014**, *47* (4), 1470−1481.

(26) Bruner, C.; Dauskardt, R. Role of Molecular Weight on the Mechanical Device Properties of Organic Polymer Solar Cells. *Macromolecules* **2014**, *47*, 1117−1121.

(27) Cranston, E. D.; Eita, M.; Johansson, E.; Netrval, J.; Salajková, M.; Arwin, H.; Wågberg, L.; Salajkov, M.; Arwin, H.; Lars, W. Determination of Young' S Modulus for Nanofibrillated Cellulose Multilayer Thin Films Using Buckling Mechanics. *Biomacromolecules* **2011**, *12* (4), 961−969.

(28) Huang, H.; Chung, J. Y.; Nolte, A. J.; Stafford, C. M. Characterizing Polymer Brushes via Surface Wrinkling. *Chem. Mater.* **2007**, *19* (26), 6555−6560.

(29) Awartani, O. M.; Zhao, B.; Currie, T.; Kline, R. J.; Zikry, M. A.; O'Connor, B. T. Anisotropic Elastic Modulus of Oriented Regioregular Poly(3-Hexylthiophene) Films. *Macromolecules* **2016**, *49* (1), 327−333.

(30) Zhao, B.; Awartani, O.; O'Connor, B.; Zikry, M. A. A Direct Correlation of X-Ray Diffraction Orientation Distributions to the in-

Plane Stiffness of Semi-Crystalline Organic Semiconducting Films. *Appl. Phys. Lett.* **2016**, *108* (18), 108−111.

(31) Kuila, B. K.; Nandi, A. K. Physical, Mechanical, and Conductivity Properties of poly(3-Hexylthiophene) -Montmorillonite Clay Nanocomposites Produced by the Solvent Casting Method. *Macromolecules* **2004**, *37* (23), 8577−8584.

(32) Kuila, B. K.; Nandi, A. K. Structural Hierarchy in Melt-Processed poly(3-Hexyl Thiophene)- Montmorillonite Clay Nanocomposites: Novel Physical, Mechanical, Optical, and Conductivity Properties. *J. Phys. Chem. B* **2006**, *110* (4), 1621−1631.

(33) Müller, C.; Goffri, S.; Breiby, D. W.; Andreasen, J. W.; Chanzy, H. D.; Janssen, R. A. J.; Nielsen, M. M.; Radano, C. P.; Sirringhaus, H.; Smith, P.; Stingelin-Stutzmann, N. Tough, Semiconducting Poly-ethylene-poly(3-Hexylthiophene) Diblock Copolymers. *Adv. Funct. Mater.* **2007**, *17* (15), 2674−2679.

(34) Printz, A. D.; Chiang, A. S. C.; Savagatrup, S.; Lipomi, D. J. Fatigue in Organic Semiconductors: Spectroscopic Evolution of Microstructure due to Cyclic Loading in poly(3-Heptylthiophene). *Synth. Met.* **2016**, *217*, 144−151.

(35) Tummala, N. R.; Risko, C.; Bruner, C.; Dauskardt, R. H.; Bredas, J. L. Entanglements in P3HT and Their Influence on Thin-Film Mechanical Properties: Insights from Molecular Dynamics Simulations. *J. Polym. Sci., Part B: Polym. Phys.* **2015**, *53* (13), 934−942.

(36) Jones, M. L.; Huang, D. M.; Chakrabarti, B.; Groves, C. Relating Molecular Morphology to Charge Mobility in Semicrystalline Conjugated Polymers. *J. Phys. Chem. C* **2016**, *120*, 4240−4250.

(37) Huang, D. M.; Faller, R.; Do, K.; Moule, A. J. Coarse-Grained Computer Simulations of Polymer/Fullerene Bulk Heterojunctions for Organic Photovoltaic Applications. *J. Chem. Theory Comput.* **2010**, *6*, 526−537.

(38) Root, S. E.; Savagatrup, S.; Pais, C. J.; Arya, G.; Lipomi, D. J. Predicting the Mechanical Properties of Organic Semiconductors Using Coarse-Grained Molecular Dynamics Simulations. *Macro-molecules* **2016**, *49* (7), 2886−2894.

(39) Lipomi, D. J.; Chong, H.; Vosgueritchian, M.; Mei, J.; Bao, Z. Toward Mechanically Robust and Intrinsically Stretchable Organic Solar Cells: Evolution of Photovoltaic Properties with Tensile Strain. *Sol. Energy Mater. Sol. Cells* **2012**, *107*, 355−365.

(40) Tahk, D.; Lee, H. H.; Khang, D.-Y. Elastic Moduli of Organic Electronic Materials by the Buckling Method. *Macromolecules* **2009**, *42* (18), 7079−7083.

(41) Awartani, O.; Lemanski, B. I.; Ro, H. W.; Richter, L. J.; DeLongchamp, D. M.; O'Connor, B. T. Correlating Stiffness, Ductility, and Morphology of Polymer:Fullerene Films for Solar Cell Applications. *Adv. Energy Mater.* **2013**, *3* (3), 399−406.

(42) O'Connor, B.; Chan, E. P.; Chan, C.; Conrad, B. R.; Richter, L. J.; Kline, R. J.; Heeney, M.; McCulloch, I.; Soles, C. L.; DeLongchamp, D. M. Correlations between Mechanical and Electrical Properties of Polythiophenes. *ACS Nano* **2010**, *4* (12), 7538−7544.

(43) Kim, J. S.; Kim, J. H.; Lee, W.; Yu, H.; Kim, H. J.; Song, I.; Shin, M.; Oh, J. H.; Jeong, U.; Kim, T. S.; Kim, B. J. Tuning Mechanical and Optoelectrical Properties of Poly(3-Hexylthiophene) through Systematic Regioregularity Control. *Macromolecules* **2015**, *48* (13), 4339−4346.

(44) Landel, R. F.; Nielsen, L. E. *Mechanical Properties of Polymers and Composites*, 2nd ed.; CRC Press: Boca Raton, FL, 1993.

(45) Johnston, I. D.; McCluskey, D. K.; Tan, C. K. L.; Tracey, M. C. Mechanical Characterization of Bulk Sylgard 184 for Microfluidics and Microengineering. *J. Micromech. Microeng.* **2014**, *24*, 35017.

(46) Selby, K.; Miller, L. Fracture Toughness and Mechanical Behaviour of an Epoxy Resin. *J. Mater. Sci.* **1975**, *10*, 12−24.

(47) Drozdov, A. D.; Christiansen, J.; de, C. Thermo-Viscoelastic and Viscoplastic Behavior of High-Density Polyethylene. *Int. J. Solids Struct.* **2008**, *45* (14−15), 4274−4288.

(48) Zen, A.; Pflaum, J.; Hirschmann, S.; Zhuang, W.; Jaiser, F.; Asawapirom, U.; Rabe, J. P.; Scherf, U.; Neher, D. Effect of Molecular Weight and Annealing of poly(3-Hexylthiophene)s on the Perform-

ance of Organic Field-Effect Transistors. *Adv. Funct. Mater.* **2004**, *14* (8), 757−764.

(49) Siddiqui, S.; Spano, F. C. H- and J-Aggregates of Conjugated Polymers and Oligomers. *Chem. Phys. Lett.* **1999**, *308* (1−2), 99−105.

(50) Spano, F. C. Modeling Disorder in Polymer Aggregates: The Optical Spectroscopy of Regioregular poly(3-Hexylthiophene) Thin Films. *J. Chem. Phys.* **2005**, *122* (23).23470110.1063/1.1914768

(51) Clark, J.; Chang, J. F.; Spano, F. C.; Friend, R. H.; Silva, C. Determining Exciton Bandwidth and Film Microstructure in Polythiophene Films Using Linear Absorption Spectroscopy. *Appl. Phys. Lett.* **2009**, *94* (16), 2007−2010.

(52) Spano, F. C.; Clark, J.; Silva, C.; Friend, R. H. Determining Exciton Coherence from the Photoluminescence Spectral Line Shape in poly(3-Hexylthiophene) Thin Films. *J. Chem. Phys.* **2009**, *130* (7), 07490410.1063/1.3076079

(53) Wohlgenannt, M.; Jiang, X. M.; Vardeny, Z. V.; Janssen, R. A. J. Conjugation-Length Dependence of Spin-Dependent Exciton Formation Rates in Π-Conjugated Oligomers and Polymers. *Phys. Rev. Lett.* **2002**, *88* (19), 197401.

(54) Karayiannis, N. C.; Kröger, M. Combined Molecular Algorithms for the Generation, Equilibration and Topological Analysis of Entangled Polymers: Methodology and Performance. *Int. J. Mol. Sci.* **2009**, *10*, 5054−5089.

(55) Shanbhag, S.; Kröger, M. Primitive Path Networks Generated by Annealing and Geometrical Methods: Insights into Differences. *Macromolecules* **2007**, *40* (8), 2897−2903.

(56) Kröger, M. Shortest Multiple Disconnected Path for the Analysis of Entanglements in Two- and Three-Dimensional Polymeric Systems. *Comput. Phys. Commun.* **2005**, *168* (3), 209−232.

(57) Hoy, R. S.; Foteinopoulou, K.; Kröger, M. Topological Analysis of Polymeric Melts: Chain-Length Effects and Fast-Converging Estimators for Entanglement Length. *Phys. Rev. E - Stat. Nonlinear, Soft Matter Phys.* **2009**, *80* (3), 14−16.